arXiv:1405.1190v1 [quant-ph] 6 May 2014

Spatial properties of twin-beam correlations at low- to high-intensity transition

Radek Machulka[1], Ondřej Haderka[2,*], Jan Peřina Jr.[1], Marco Lamperti,[3] Alessia Allevi,[3,4] and Maria Bondani[5,4]

[1] *RCPTM, Joint Laboratory of Optics of PU and Inst. Phys. AS CR, 17. listopadu 12, 77146 Olomouc, Czech Republic*

[2] *Institute of Physics AS CR, Joint Laboratory of Optics, 17. listopadu 50a, 77146 Olomouc, Czech Republic*

[3] *Dipartimento di Scienza e Alta Tecnologia, Università degli Studi dell'Insubria, Via Valleggio 11, 22100 Como, Italy*

[4] *CNISM UdR Como, via Valleggio 11, 22100 Como, Italy*

[5] *Istituto di Fotonica e Nanotecnologie, CNR, Via Valleggio 11, 22100 Como, Italy*

[*] *ondrej.haderka@upol.cz*

Abstract: It is shown that spatial correlation functions measured for correlated photon pairs at the single-photon level correspond to speckle patterns visible at high intensities. This correspondence is observed for the first time in one experimental setup by using different acquisition modes of an intensified CCD camera in low and high intensity regimes. The behavior of intensity auto- and cross-correlation functions in dependence on pump-beam parameters including power and transverse profile is investigated.

© 2014 Optical Society of America

OCIS codes: (190.4410) Nonlinear optics, parametric processes; (270.0270) Quantum optics; (230.5160) Photodetectors.

References and links

1. L. Mandel and E. Wolf, *Optical Coherence and Quantum Optics* (Cambridge University, 1995).
2. A. A. Malygin, A. N. Penin, and A. V. Sergienko, "Spatiotemporal grouping of photons in spontaneous parametric scattering of light," Dokl. Akad. Nauk SSSR **281**, 308–313 (1985).
3. B. M. Jost, A. V. Sergienko, A. F. Abouraddy, B. E. A. Saleh, and M. C. Teich, "Spatial correlations of spontaneously down-converted photon pairs detected with a single-photon-sensitive CCD camera," Opt. Express **3**, 81–88 (1998).
4. A. Mosset, F. Deveaux, G. Fanjoux, and E. Lantz, "Direct experimental characterization of the Bose-Einstein distribution of spatial fluctuations of spontaneous parametric down-conversion," Eur. Phys. J. D **28**, 447–451 (2004).
5. O. Haderka, J. Peřina Jr., M. Hamar, "Simple direct measurement of nonclassical joint signal-idler photon-number statistics and the correlation area of twin photon beams," J. Opt. B - Quantum Semicl. Opt. **7**, S572–S576 (2005).
6. M. P. Edgar, D. S. Tasca, F. Izdebski, R. E. Warburton, J. Leach, M. Agnew, G. S. Buller, R. W. Boyd, and M. J. Padgett, "Imaging high-dimensional spatial entanglement with a camera", Nat. Commun. 3:984 (2012).
7. C. H. Monken, P. H. Souto Ribeiro, and S. Padua, "Transfer of angular spectrum and image formation in spontaneous parametric down-conversion," Phys. Rev. A **57**, 3123–3126 (1998).
8. G. Molina-Terriza, S. Minardi, Y. Deyanova, C. I. Osorio, M. Hendrych, and J. P. Torres, "Control of the shape of the spatial mode function of photons generated in noncollinear spontaneous parametric down conversion," Phys. Rev. A **72**, 065802 (2005).
9. T. P. Grayson and G. A. Barbosa, "Spatial properties of spontaneous parametric down-conversion and their effect on induced coherence without induced emission," Phys. Rev. A **49**, 2948–2961 (1994).
10. A. Joobeur, B. E. A. Saleh, and M. C. Teich, "Spatiotemporal coherence properties of entangled light beams generated by parametric down-conversion," Phys. Rev. A **50**, 3349–3361 (1994).

11. A. Joobeur, B. E. A. Saleh, T. S. Larchuk, and M. C. Teich, "Coherence properties of entangled light beams generated by parametric down-conversion: theory and experiment," Phys. Rev. A **53**, 4360–4371 (1996).
12. M. Hamar, J. Peřina Jr., O. Haderka, and V. Michálek, "Transverse coherence of photon pairs generated in spontaneous parametric downconversion," Phys. Rev. A **81**, 043827(2010).
13. E. Brambilla, A. Gatti, M. Bache, and L. A. Lugiato, "Simultaneous near-field and far-field spatial quantum correlations in the high-gain regime of parametric down-conversion," Phys. Rev. A **69**, 023802 (2004).
14. M. Bondani, A. Allevi, and A. Andreoni, "Ghost imaging by intense multimode twin beam," Eur. Phys. J. Special Topics **203**, 151–161 (2012).
15. O. Jedrkiewicz, Y.-K. Jiang, E. Brambilla, A. Gatti, M. Bache, L. A. Lugiato, and P. Di Trapani, "Detection of sub-shot-noise spatial correlation in high-gain parametric downconversion," Phys. Rev. Lett. **93**, 243601 (2004).
16. G. Brida, M. Genovese, A. Meda, E. Predazzi, and I. Ruo Berchera, "Systematic study of the PDC speckle structure for quantum imaging applications," Int. Journ. Quantum Inf. **7**, 139–147 (2009).
17. G. Brida, M. Genovese, A. Meda, E. Predazzi, and I. Ruo Berchera, "Tailoring PDC speckle structure," J. Mod. Opt. **56**, 201–208 (2009).
18. J. Peřina Jr., O. Haderka, V. Michálek and M. Hamar, "Absolute detector calibration using twin beams," Opt. Lett. **37**, 2475–2477 (2012).
19. X. Y. Zou, L. J. Wang and L. Mandel, "Induced coherence and indistinguishability in optical interference," Phys. Rev. Lett. **67**, 318—321 (1991).
20. J. Peřina Jr., "Spatial properties of entangled photon pairs generated in nonlinear layered structures," Phys. Rev. A **84**, 053840 (2011).

1. Introduction

Optical twin-beams generated by spontaneous parametric down-conversion (PDC) are well known to exhibit temporal and spatial correlations [1]. The first experimental measurements of spatial correlations in twin beams, aimed at determining the size of the coherence areas in the transverse planes, date back to 1990s [2, 3] and early 2000s [4, 5]. Such measurements were performed in the single-photon regime on twin-beams containing one photon at most by using scanned single-photon detectors (photomultipliers operating in Geiger mode [2], avalanche photodiodes [7, 8]), intensified CCDs [3, 5] or EMCCDs [6]). The experimental results can be compared to a well established theory properly working in this regime [9-12].

On the other hand, twin-beam states can also be generated in a much higher intensity regime [13], in which coherence areas become visible in single-shot images [14, 15]. In the high-gain parametric process, the sizes of the coherence areas exhibit dependence on the gain [15]. The quantification of the size of coherence areas can be obtained through intensity auto- (AC, Γ_{ss}, Γ_{ii}) and cross-correlation (XC, Γ_{si}, Γ_{is}) functions [16, 17] defined as

$$\Gamma_{ab}(\mathbf{r}_1,\mathbf{r}_2) = \langle \Delta I_a(\mathbf{r}_1)\Delta I_b(\mathbf{r}_2)\rangle, \quad a,b = s,i. \tag{1}$$

Symbol s [i] stands for a signal [idler] beam with intensity fluctuation $\Delta I_s(\mathbf{r}_1)$ [$\Delta I_i(\mathbf{r}_2)$] at position $\mathbf{r}_1$ [$\mathbf{r}_2$] and $\langle\rangle$ denotes quantum (statistical) averaging. Although the two described intensity regimes together with their own experimental techniques differ considerably, the observed effects arise from the same nonlinear process. That is why it is important to compare quantitatively the observed coherence properties at single-photon and intense twin-beam regime.

In a recent publication [12] we explored in detail spatial coherence of twin beams at single-photon level by using photon-counting methods. As the detector we used a single-photon sensitive intensified CCD camera illuminated by a PDC field containing much less than one photon per active superpixel and detection interval of the camera. In particular, we have shown that the transverse coherence functions of twin beams can be tailored by changing the pump-beam properties.

In this paper, we investigate the above mentioned regime hand in hand with the intense twin-beam regime containing formed speckles. In the latter regime, the PDC field is so intense that many photons impinge on each superpixel of the camera during the detection interval. As a consequence, the camera amplification is tuned down and the camera loses its single-photon

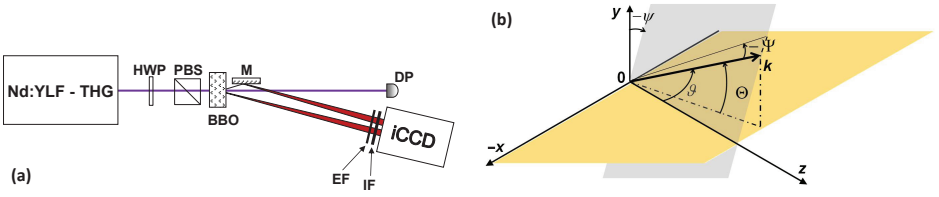

Fig. 1. (a) Sketch of the experimental setup (see text for details). (b) Propagation geometry of a plane wave with wave vector $\mathbf{k}$ in the reference frame of the crystal: ϑ is the radial angle measured from the z axis in the incidence plane and ψ is the azimuthal angle that gives the rotation of the plane of incidence with respect to the plane yz. Alternatively, the coordinate system of the camera is used: Θ is the radial angle measured in the plane perpendicular to the xz plane from the intersection of the two planes and Ψ is the azimuthal angle in the plane perpendicular to the plane of angle Θ.

sensitivity and provides only classical field intensities. Nevertheless, the intensity XC functions evaluated from intensity measurements correspond to those measured by the photon-counting technique at the single-photon level. Moreover, the dependence of both intensity AC and XC functions on pump-beam parameters fits with that observed at single-photon level and predicted by theory.

2. Experimental setup

Our experiment was performed by using the third-harmonics (349 nm) of a ps-pulsed mode-locked Nd:YLF laser (High-Q Laser) to pump a 8-mm-long BBO crystal ($\theta = 37°$). Nearly degenerate photon pairs occurred at a cone layer with a vertex half-angle of 11.9°. A part of the cone layer was selected by a 40-nm-wide bandpass interference filter (IF) centered at 710 nm, that is close to frequency degeneracy. One part of the cone-layer (signal) was captured directly by the photocathode of the iCCD camera (Andor DH734, pixel size 13×13 μm^2) placed 38.5 cm behind the crystal, while the corresponding twin portion (idler) was directed to a different section of the photocathode using a dielectric mirror (M, see Fig. 1). An additional long-pass filter (EF) was used to cut scattered pumping photons. The camera was triggered by an electronic pulse derived from the laser pulse and set to 5 ns detection window (used both for low- and high-intensity measurement) to assure detection of PDC from a single pump pulse and to minimize noise. The power of the transmitted pump beam was monitored using a power-meter. Moreover, the pump beam diameter was measured in the horizontal and vertical directions using a scanning knife-edge. The pump beam was nearly elliptical with the vertical width reaching approximately 70% of the horizontal one. The pump power was changed by using a half-wave plate (HWP) followed by a polarizing beam splitter.

3. Results

First of all, we measured the correlation area characterizing intensity XC function in the transverse plane by exploiting the photon-counting method presented in [12]. We took a long sequence of camera frames [see Figs. 2(a) and 2(b)] and processed them in the way described in [5]. The camera was set to its maximum gain and a 8x8-hardware binning was used to speed up the acquisition. In each frame of the sequence, single-photon detection events have been identified separately for the signal and idler regions after thresholding above the readout noise of the CCD chip. Since the number of binned superpixels (> 6000) is much larger than the number of incident photons, the impinging probability is well below one photon per superpixel and the camera serves in fact as two (signal and idler) photon-number-sensitive detectors in this regime.

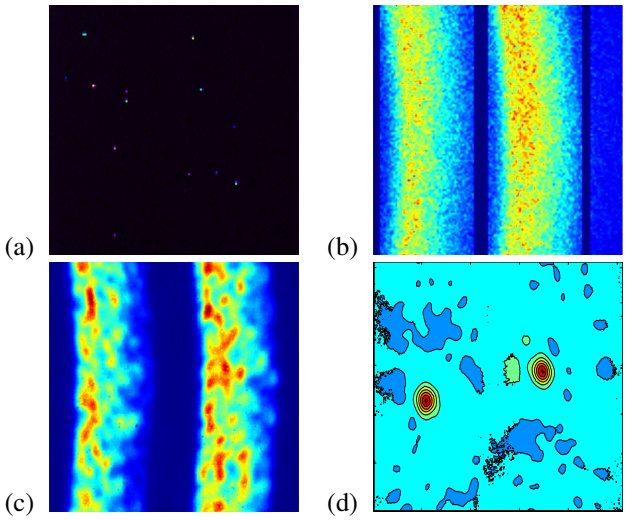

Fig. 2. Typical images taken by the iCCD camera in the experiment. a) single frame at the single-photon level ($P_p = 20$ μW). b) summed image of frames at the single-photon level with the overall mean photon number equal to that in c); c) single frame at the mesoscopic level with speckles ($P_p = 45$ mW). d) intensity AC and XC functions computed from a sequence of 1000 frames taken at classical intensity. Two peaks appear in the image: the left peak is located around the selected idler point, thus describing the intensity AC function Γ_{ii}. The right peak is centered at the conjugate signal point given by ideal phase-matching conditions, thus giving the intensity XC function Γ_{is}. The axes are scaled in superpixels of the iCCD.

Using the whole sequence, correlations of detection-event positions are obtained as well as first and second moments of the photocount distributions. From these data we can get the correlation area with a full-width half maximum (FWHM) of $\Delta\Gamma_{is,\Theta} = (490 \pm 52)$ μm in the horizontal direction (radial with respect to the cone section) and $\Delta\Gamma_{is,\Psi} = (710 \pm 52)$ μm in the vertical (azimuthal) one. The sequence was measured at the pump power $P_p = 20$ μW, which resulted in 8.9 mean idler detected photons and 10.5 mean signal detected photons. As our method naturally includes also the determination of effective quantum detection efficiency [18], we could assign 7.2% and 8.5% detection efficiency to idler and signal beams, respectively. We ascribe this difference to the non-perfect reflectivity of the mirror in the idler path.

The increase of pump power P_p causes the transition from photon-counting to classical-intensity measurement and patterns with speckles [see Fig. 2(c)] occur in single-shot images for P_p values larger than 20 mW. By setting a 4x4-hardware binning, we took a sequence of 1000 images for different pump powers and pump-beam sizes and processed them by computing intensity AC functions Γ_{ii} and XC functions Γ_{is} at 100 randomly selected points in the fringe patterns close to the frequency degeneracy of the PDC process [for an example, see Fig. 2(d)]. This approach gives a better signal-to-noise ratio than taking the correlation of the whole image, as only a part of the image is covered by a significant light intensity. These correlation functions are conveniently characterized by their horizontal $\Delta\Gamma_\Theta$ and vertical $\Delta\Gamma_\Psi$ widths that depend on pump-beam parameters.

The character of the observed speckle patterns remains stable in the range between 30 mW and 50 mW of the pump power P_p, as shown in Fig. 3. The width $\Delta\Gamma$ of intensity XC function both in the radial [Fig. 3(a)] and azimuthal [Fig. 3(b)] directions is systematically larger than the corresponding width of the intensity AC function. This occurs probably due to the geometry

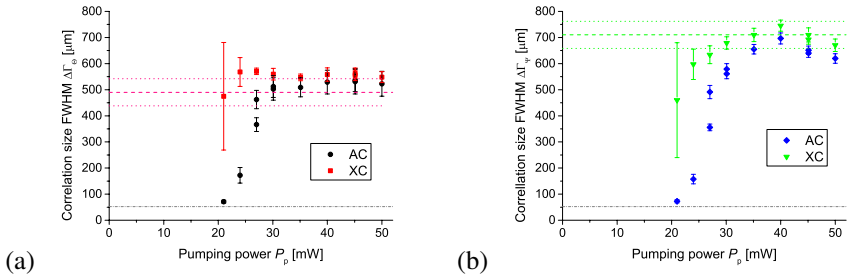

Fig. 3. (a) Radial width $\Delta\Gamma_\Theta$ and (b) azimuthal width $\Delta\Gamma_\Psi$ of intensity AC (rectangles) and XC (circles) functions (FWHM) depending on pump power P_p. Dashed lines correspond to the XC function width $\Delta\Gamma$ measured at power $P_p = 20$ μW by the photon-counting approach (dotted lines define the standard deviation of measurement). The bottom dash-dot line shows the size of the macropixel used in the measurements.

of our experiment which is not perfectly far-field as we do not use any imaging to simplify the setup. The drop in AC function widths $\Delta\Gamma$ occurring for low pump powers P_p (below 30 mW) reflects insufficient coherence inside the field observed for not sufficiently intense stimulated process. The width of the XC function Γ_{is} remains large in this region, as the coherence between the signal and idler fields (XC) originates in spontaneously generated photon pairs whereas the internal coherence (AC) of both emitted beams arises from stimulated emission in the nonlinear process [19]. Below 20 mW, the AC correlation-function widths are already at the level of a single macropixel of the detector and bear no other physical meaning than the pixelization of the detector. The dashed line in Fig. 3 is drawn at the value of XC function width $\Delta\Gamma_{is}$ measured at the single-photon level ($P_p = 20$ μW). We can see that its value coincides well with the widths $\Delta\Gamma_{is}$ of the correlation functions obtained by classical-intensity measurements. This gives an experimental evidence that the correlation functions obtained in single-photon and classical-intensity measurements represent the same physical phenomenon of PDC though observed at different physical conditions. Whereas the twin beams at single-photon level are described by highly nonclassical multi-mode Fock states with completely random optical phases, the intense twin beams are well described by multi-mode classical coherent states whose well defined phase properties inside individual modes manifest themselves with the occurrence of speckles[13].

Close similarity in the behavior of intensity correlation functions in both regimes has been experimentally confirmed by observing the behavior of correlation size as a function of the pump-beam diameter w_p. As shown in [12], the intensity XC function is sensitive to the pump-beam diameter w_p inside the nonlinear crystal, especially in the azimuthal direction. For this reason, we have investigated this dependence in the classical-intensity regime (see Fig. 4). In agreement with our previous results obtained at the single-photon level [12], the radial widths $\Delta\Gamma_\Theta$ of both intensity AC and XC functions do not significantly depend on the pump-beam diameter w_p. This is caused by the fact that the phase-matching condition along the propagation z axis is much more restrictive for the used BBO crystal than the phase-matching condition in the transverse plane related to the radial direction that encompasses the pump-beam spatial spectrum[12] (see Fig. 4). On the other hand, a roughly hyperbolic dependence of the widths $\Delta\Gamma_\Psi$ of intensity correlation functions on pump-beam diameter w_p has been observed in the azimuthal direction [see Fig. 4]. This dependence arises from the phase-matching condition along the azimuthal direction, which crucially depends on the corresponding pump-beam spatial spectrum. The wider the pump-beam spatial spectrum the less strict the phase-matching conditions and so the wider the observed widths. Also theoretical predictions for the widths

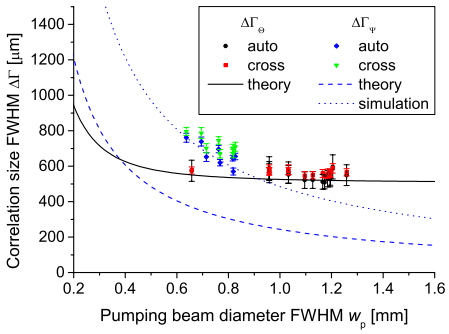

Fig. 4. Width $\Delta\Gamma_{ii}$ of intensity AC functions (circles, triangles) and $\Delta\Gamma_{is}$ of XC functions (rectangles, diamonds, FWHM) as they depend on pump-beam diameter w_p. Radial (circles, rectangles) and azimuthal (triangles, diamonds) dependencies are shown simultaneously. Azimuthal widths $\Delta\Gamma_\Psi$ are plotted against vertical pump beam diameter w_p while radial widths $\Delta\Gamma_\Theta$ are drawn against horizontal pump-beam diameter w_p. The placement of the azimuthal points at lower values of w_p stem from ellipticity of the pump beam. Solid (radial) and dashed (azimuthal) curves are based on a theoretical model [20]. Dotted line shows a theoretical curve for a pumping beam with spatial spectrum twice wider than an ideal Gaussian beam (see the text).

$\Delta\Gamma$ of intensity correlation functions are drawn in Fig. 4. They were obtained by the model that decomposes the interacting fields into plane waves, uses Gaussian pump temporal and spatial spectral profiles and considers phase-matching conditions for the wave vectors along all three directions (for more details, see [20]). As it follows from Fig. 4, both experimental data and theoretical curves are in qualitative agreement. However, a complicated multi-mode spatial structure of the intense pump beam that was difficult to monitor and control in the experiment did not allow us to model the nonlinear process with the sufficient precision needed for finding a better agreement. The complicated pump-beam structure in its transverse plane results in a spatial spectrum wider and richer than the Gaussian spectrum considered in the model. As a consequence, the experimental widths of intensity correlation functions in azimuthal direction are wider (see dotted line in Fig. 4 for an example of the effect of a wider spatial spectrum).

4. Conclusion

We have shown that intensity correlation functions of twin beams measured at single-photon level correspond to those of twin beams with speckle patterns reached at high intensities. The single-photon and high-intensity XC functions are equal as the mutual coherence of signal and idler fields arises from the generation of photon pairs. On the contrary, internal coherence of both fields originates from stimulated emission and so AC functions drop down to zero for weak fields. The obtained experimental dependencies of intensity AC and XC functions of intense speckle fields on pump-beam parameters and their comparison with the corresponding single-photon counterparts have confirmed this correspondence.

Acknowledgments

Support by projects P205/12/0382 of GA ČR and projects CZ.1.05/2.1.00/03.0058 and CZ.1.07/2.3.00/20.0058 of MŠMT ČR are acknowledged. RM thanks to IGA PrF_2014_005. The support of MIUR (FIRB LiCHIS - RBFR10YQ3H) is also acknowledged.